High-Temperature Sulfidation of NiCoCrAl(Y) Alloys

E. Godlewska[1], E. Roszczynialska[1] and Z. Żurek[1,2]

[1]*Department of Solid State Chemistry, St. Staszic University of Mining & Metallurgy, Al. Mickiewicza 30, 30059 Cracow, Poland.*

[2]*Institute of Inorganic Chemistry & Technology, Cracow University of Technology, ul. Warszawska 24, 31155 Cracow, Poland.*

ABSTRACT

Sulfidation of an alloy having a nominal composition Ni-23Co-19Cr-12Al (wt%) with and without the addition of 0.6% yttrium was studied at a temperature of 1173 K and a sulfur vapor pressure of 10^5Pa. The sulfidation run was followed thermogravimetrically. Phase and chemical composition of sulfide scales and scale morphologies were analyzed after different time intervals. Sulfidation rates of both alloys proceeded at comparable rates. The sulfide scales showed complex microstructures and compositions, with several sulfospinel phases present and distinct stratification after longer reaction times. There was no evidence of yttrium segregation either to the grain boundary regions in the scale or to the alloy/scale interface. Yttrium dissolution in the sulfide phases (doping effect) distinctly affected scale microstructure.

1. INTRODUCTION

In spite of the fact that an intensive search for alternative structural materials has been going on during the last few years, it does not seem very likely that high-temperature, high-strength superalloys will easily give way to the successors. The temperature/ pressure/environmental hazards imposed by modern technologies call for efficient and reliable protection systems for the load-bearing parts. Among a great variety of the protective systems used to increase scaling resistance of superalloys, the overlay MCrAl(X) coatings (with M = Ni, Co and X = Y, Zr, H, Ta, Ti, etc.) offer an advantage of appreciable compositional flexibility.

The aluminum and rare-earth additions provide good oxidation resistance, whereas relatively high chromium levels ensure hot-corrosion resistance. Compositional modification of the overlay coatings, particularly of the Cr:Al ratio, makes them suitable for a variety of service conditions. Oxidation and hot-corrosion behavior of the MCrAl(X) materials, alone or deposited on superalloy substrates, have been a subject of many investigations /1-15/, whereas their sulfidation behavior as well as phase equilibria in multicomponent metal-sulfur systems are less known.

The purpose of this work was to obtain information on high-temperature corrosion of NiCoCrAl(Y) alloys in sulfur vapor from the viewpoint of reaction kinetics as well as scale structure and composition.

2. EXPERIMENTAL

The alloys having the nominal compositions Ni-23Co-19Cr-12Al and Ni-23Co-19Cr-12Al-0.6Y (wt.%) were obtained by vacuum melting of pure metals (99.99%) followed by vacuum annealing at 1173 K for 48 h. Chemical compositions of the starting materials are given in Table 1. The ingots were spark-machined to get flat disks, 15 mm in diameter and 0.8 mm thick, which were ground on SiC-papers up to 800 grit no.,

Table 1
Chemical composition of starting materials (wt.%)

Element	NiCoCrAl	NiCoCrAl+Y
Co	22.8	22.7
Cr	19.0	18.9
Al	12.0	11.9
Y	—	0.62
Si	0.08	0.10
C	0.013	0.018
S	0.0008	0.0004
P	0.001	0.001
Fe	0.12	0.12
O	0.0059	0.0064
N	0.0124	0.0090
Ni	bal	bal

then polished with 1 μm diamond paste and finally degreased in water with detergent and ultrasonically cleaned in acetone.

The analyses of phase and chemical compositions of starting materials by XRD, EDX and EPM as well as optical and scanning electron microscope observations revealed that these materials were heterogeneous and consisted of a fcc γ-Ni enriched in cobalt and chromium and a bcc β-(Ni,Co)Al intermetallic compound. The NiCoCrAlY alloy contained in addition M_5Y-type precipitates having the composition $Ni_{3.55}Co_{0.5}Cr_{0.2}Al_{0.75}Y$. Alloy microstructures are shown in Figs. 1a and 1b.

The sulfidation experiments were carried out at a temperature of 1173 K and sulfur vapor pressure of 10^5Pa in a thermogravimetric assembly, described elsewhere /16/, enabling continuous registration of weight gains, with an accuracy of 10^5g. The sulfur vapor at atmospheric pressure was delivered from the sulfur reservoir located at the bottom of the reaction tube and kept at the boiling point of sulfur. The sulfidation runs were continued for 12 and 24 hrs. Selected samples were additionally subjected to short-term sulfidation experiments in order to elucidate possible stages of scale development.

The chemical and phase compositions of sulfidized specimens were analyzed with the aid of XRD (diffraction patterns taken from the top and bottom of the detached scales + powder patterns of scales, diffraction patterns taken from the subscale surface of metallic core), EDX (fracture sections), EPM (cross-sections).

3. RESULTS AND DISCUSSION

The results of thermogravimetric measurements for

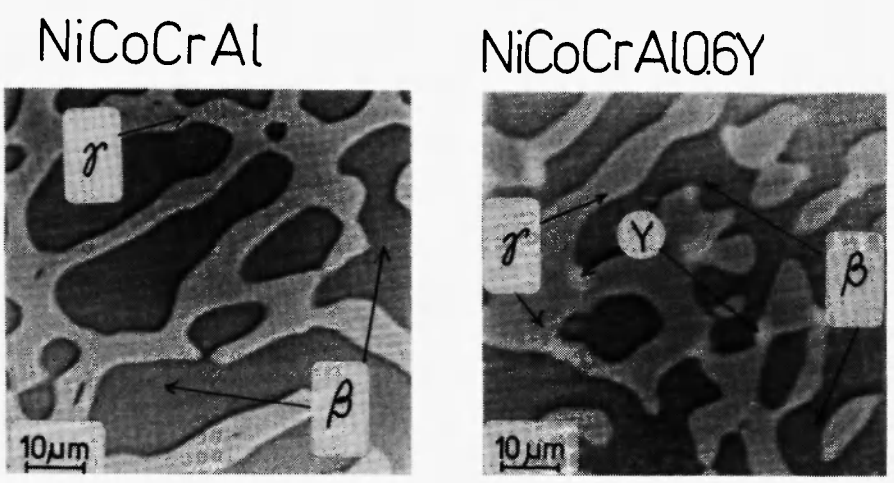

Fig. 1: Microstructures of starting materials a) NiCoCrAl, b) NiCoCrAlY.

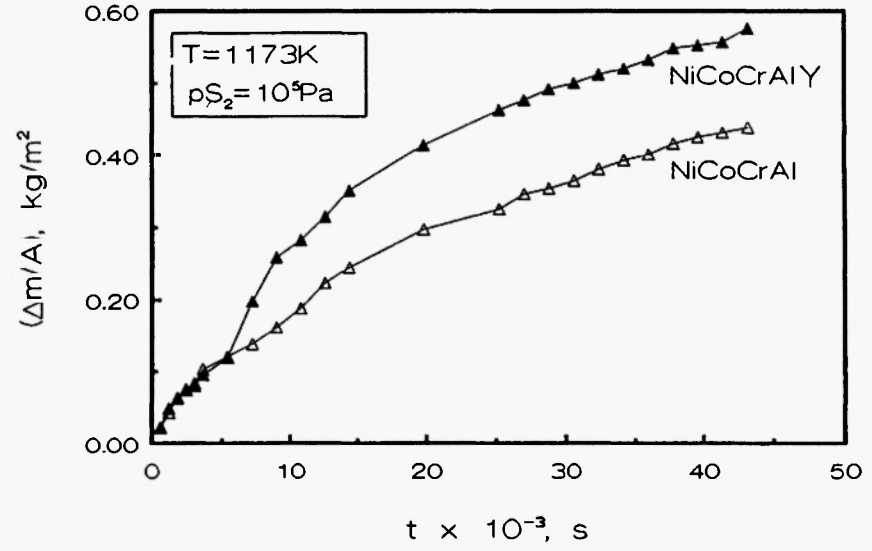

Fig. 2: Sulfidation of NiCoCrAl and NiCoCrAlY alloys at 1173K and $pS_2 = 10^5$Pa (12-h runs).

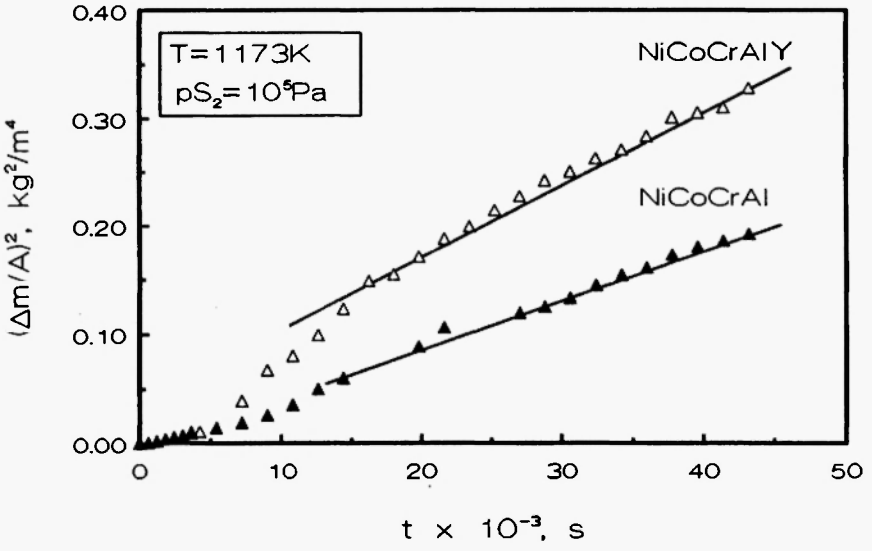

Fig. 3: Sulfidation of NiAlCr(Y) alloys in a parabolic plot (12-h runs).

both materials studied in 12- and 24-h sulfidation runs are shown in Figs. 2-4. It is seen that the weight gains of the yttrium-free alloy are slightly smaller than those of yttrium-containing alloy, which is in contrast to the results reported in the literature for materials of similar composition sulfidized at 973 K and sulfur pressure of 10^4Pa /17/. For the 12-h runs, the sulfidation rates of both materials (expressed as tangents of the kinetic curve) decrease with time, which may reflect diffusion control of sulfide scale growth. As can be seen in Fig. 3 presenting the measured weight gains versus time in a parabolic plot, after an initial period of about 2 hours, the sulfidation process obeys a parabolic rate law, with the estimated sulfidation rates of the order of 10^{-6} kg^2/m^4s. In contrast, for the 24-h runs (Fig. 4), the kinetic curves assume a step-like shape indicating transient accelerations, the origin of which will be explained later after detailed examination of scale structure and composition.

Sulfide scales formed on both materials under investigation are heterogeneous and layered, as shown in Fig. 5. Examination of EDX spectra taken at

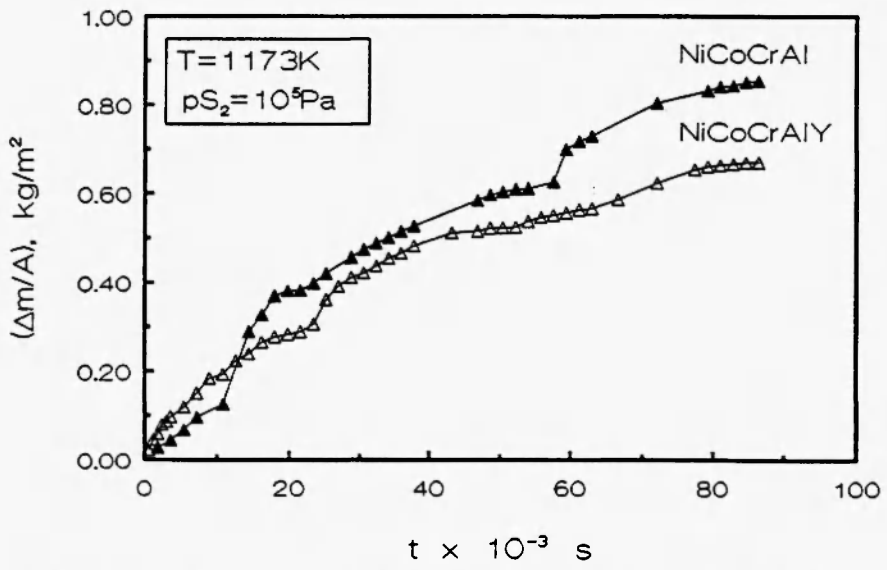

Fig. 4: Sulfidation of NiCoCrAl and NiCoCrAlY alloys at 1173K and $pS_2 = 10^5$Pa (24-h runs).

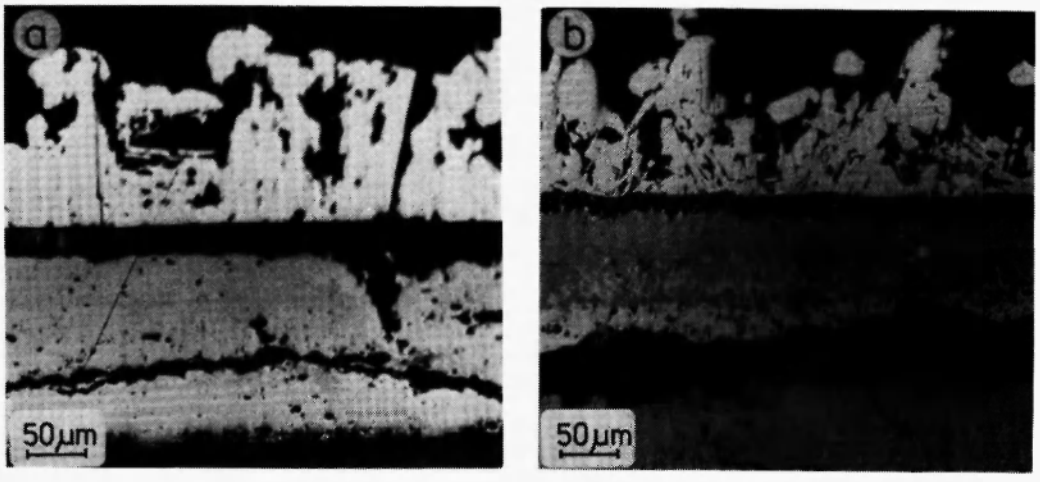

Fig. 5: Cross-sections of sulfide scales on NiCoCrAl a) 12 h, b) 24 h runs.

different points of fracture sections indicates that nickel and cobalt concentrations are highest in the outermost part of the scale, whereas those of aluminum and chromium increase in the subjacent scale layers. This observation is supported by the concentration profiles of elements across the scale/alloy interface taken from transversal cross-sections of the sulfidized specimens, as shown in Figs. 6 and 7. The results of EDX and EPM analyses in conjunction with the obtained XRD patterns indicate that the outermost scale layer is built of (Ni,Co)S or $(Ni,Co)_3S_4$ + (Ni,Co)S depending on the duration of the sulfidation process, the intermediate one is $(Co,Ni)Al_2S_4$, and the innermost - $(Cr,Ni,Co)Al_2S_4$ (Figs. 8, 9). It is worthwhile mentioning that aluminum sulfide, being the most stable sulfide phase in the investigated system, has not been detected in the scale. This, however, is typical of relatively fast sulfidation processes /18-25/. The appearance of an internal sulfidation zone (Fig. 10) indicates that in the two-phase structure of the alloy neither of the phases is consumed preferentially, the sulfidation front being reasonably uniform. In contrast to the extensively studied oxidation processes of yttrium-modified materials, yttrium segregation has not been detected in

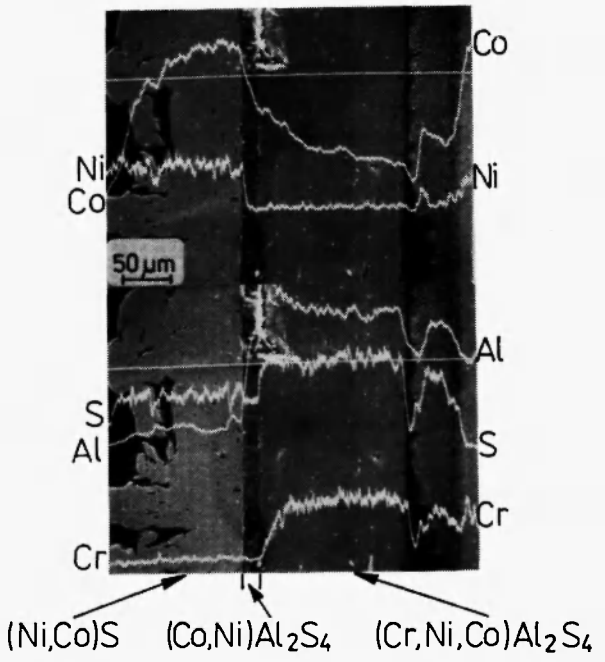

Fig. 6: Micrograph of scale cross-section on NiCoCrAl with concentration profiles of elements along the marked line.

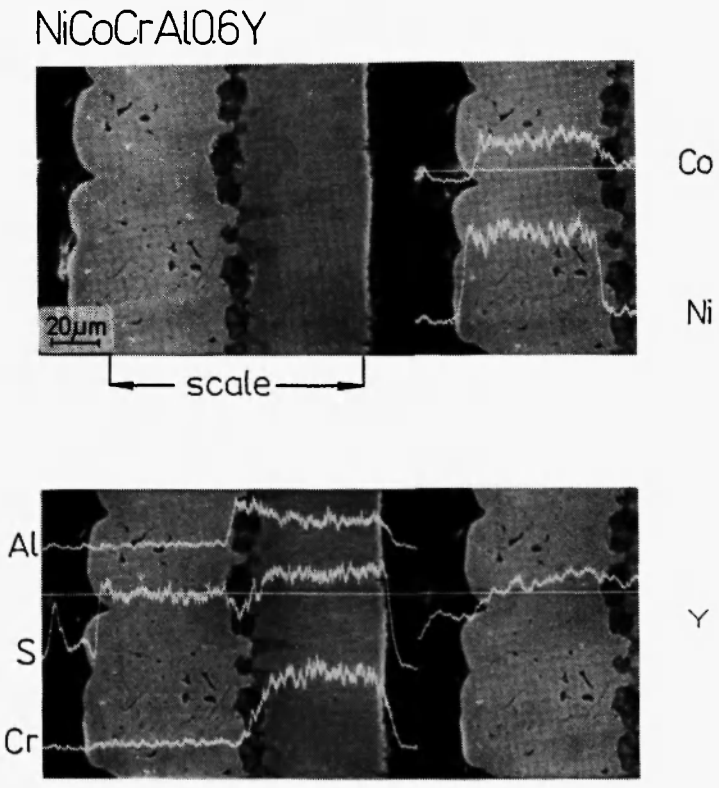

Fig. 7: Micrograph of scale cross section on NiCoCrAlY with concentration profiles of elements along the marked line.

the grain boundary region of the sulfide scale or at the alloy/scale interface (see Fig. 7). Yttrium effect is, however, visible in scale microstructure, especially in the outermost "nickel sulfide" layer. After different reaction times this layer appears more compact and massive, although its overall thickness is approximately the same as that on the yttrium-free alloy (Fig. 11). This observation can be ascribed to the doping effect of yttrium in the nickel sulfide scale. Nickel sulfide, NiS, is defective within the cation sublattice, predominant defects being cation vacancies and electron holes. Substitution of trivalent yttrium ions in nickel lattice sites introduces additional ionic defects – cation vacancies. An increasing concentration of cation vacancies can also be expected if the trivalent yttrium ion enters the structure of the cation-deficient chromium-aluminum sulfospinel /26/, although due to simultaneous dissolution of nickel and cobalt the effect is not very clear. Going back to the specific shape of kinetic curves observed in 24-h runs (Fig. 4), one can find a correlation between their step-like character and the stratified structure of the scale. As can be seen in Fig. 5, there are two sequences of layers having essentially the same compositions. Since compositional fluctuations in the gas atmosphere (flowing sulfur vapor) were impossible and those of the underlying alloy were not observed, the transient acceleration of the sulfidation process could be accounted for by detachment of the primary scale along the scale/alloy interface and growth of another scale layer on the surface of metallic core, involving inward transport of sulfur through microcracks and fissures in the earlier formed scale. This process is accompanied by secondary reactions between both scale layers which bring about their "fusion" and a very peculiar appearance. A similar stratified structure of sulfide scale has been reported for a NiAl-20Cr (at.%) pseudobinary alloy sulfidized in sulfur vapor at $2*10^3$Pa and a temperature of 1173 K /27/. It seems that the qualitative model of scale growth schematically shown in Fig. 12 can be used to explain the sulfidation behavior of NiCoCrAl(Y) alloys at high sulfur pressures. In this model it is assumed that each scale layer grows due to

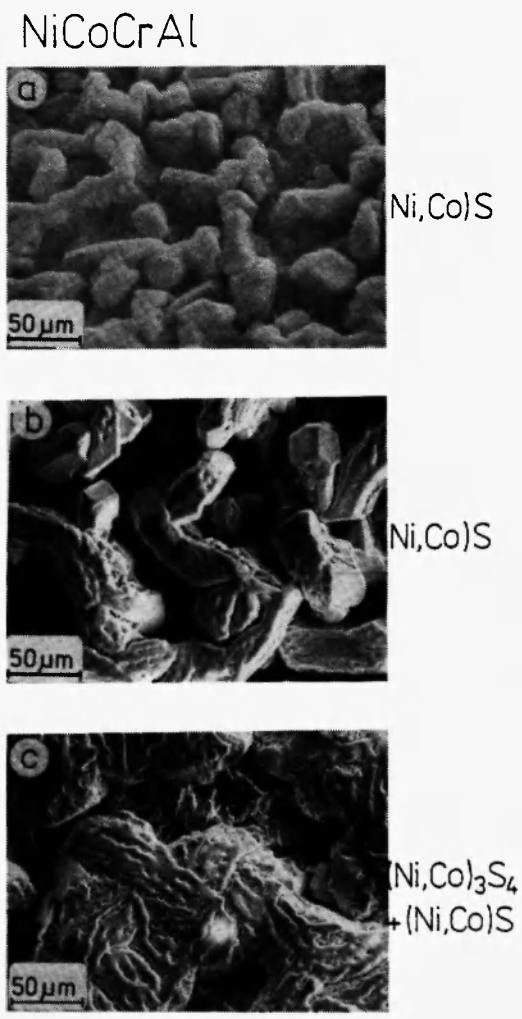

Fig. 8: Micrographs of sulfide scale surface on NiCoCrAl substrate after different reaction times: a) 1.5 h, b) 12 h, c) 24 h.

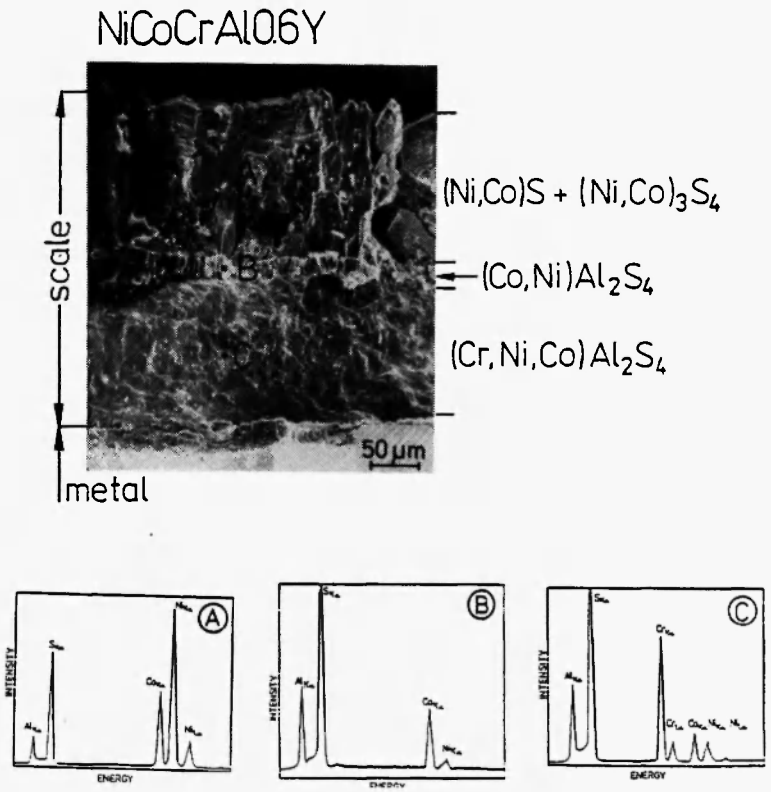

Fig. 9: Fracture section of sulfide scale on NiCoCrAlY sample (sulfidation time 24 h).

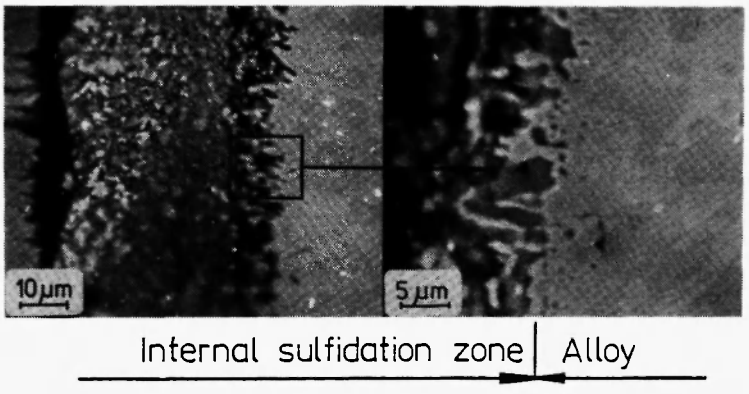

Fig. 10: Internal sulfidation zone on NiCoCrAl alloy sulfidized 20 h.

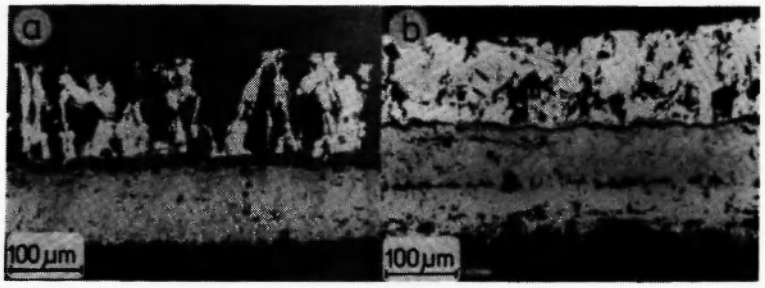

Fig. 11: Cross-sections of sulfide scales on a) NiCoCrAl and b) NiCoCrAlY alloys (sulfidation time 16 h).

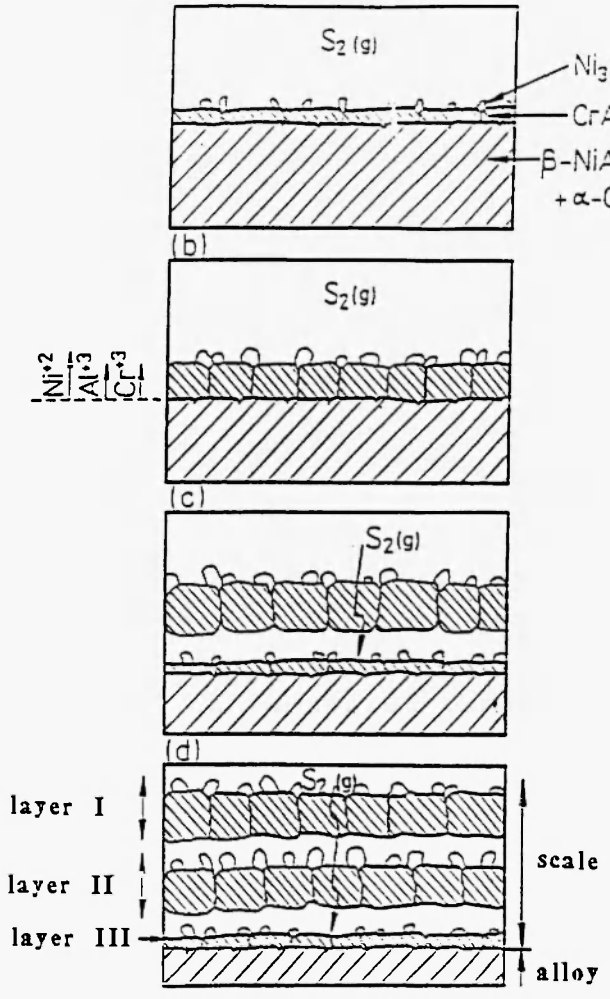

Fig. 12: Development of stratified scale on NiAl-20Cr alloy sulfidized in sulfur vapor /27/.

the outward diffusion of cations up to the moment when some critical thickness is attained, dependent on sample geometry and sulfidation conditions, then it loses contact with the metallic core. This happens most probably as a result of mechanical stresses generated in the growing scale and lack of thermodynamic equilibrium at the scale/alloy interface (retarded nucleation of aluminum sulfide). In addition to the physical separation at the scale/alloy interface, cracks or microfissures appear within the scale, enabling sulfur penetration toward the metallic core. As a result of these processes another scale layer develops on the alloy surface and again grows predominantly due to the outward diffusion of cations.

4. SUMMARY

Sulfidation of NiCoCrAl(Y) alloys at a temperature of 1173 K and a sulfur pressure of 10^5Pa follows approximately a parabolic rate law only at short reaction times, with the estimated sulfidation rates of the order of 10^{-6}kg^2/m^{4}s. Further sulfidation involves secondary reactions reflected in a step-like shape of kinetic curves and scale stratification. The sulfide scales have complex compositions and microstructures, with several sulfospinel phases present, such as $(Ni,Co)_3S_4$, $(Co,Ni)Al_2S_4$ and $(Cr,Ni,Co)Al_2S_4$. Yttrium dissolves in the sulfide phases, bringing about changes in scale microstructure and slightly modifying the sulfidation rate.

ACKNOWLEDGEMENTS

This work has been carried out under contract no. 10.160.91 financed by the Polish Committee for Scientific Research and Development (KBN).

REFERENCES

1. F.J. Pennisi and D.K. Gupta, *Thin Solid Films*, 84, 49 (1981).
2. S.J. Shaffer, D.H. Boone, R.T. Lambertson and D.E. Peacock, *Thin Solid Films*, **107**, 463 (1983).
3. A.R. Nicoll and G. Wahl, *Thin Solid Films*, 95, 21 (1982).
4. H.W. Grunling and R. Bauer, *Thin Solid Films*, 95, 3 (1982).
5. M. Frances, M. Vilasi, M. Mansour-Gabr, J. Steinmetz and P. Steinmetz, *Mat. Sci. & Eng.*, 88, 89 (1987).
6. M. Vilasi, M. Mansour-Gabr, J. Steinmetz and P. Steinmetz, *Met. Sci. & Eng.*, **96**, 247 (1987).
7. D.K. Gupta and D.S. Duvall, in: "Superalloys 1984", Proc. of the Fifth International Symposium on Superalloys, Oct. 7-11, 1984, Seven Springs, Champion, PA, U.S.A., p. 711.
8. A.R. Nicoll and G. Wahl, *ibid.*, p. 805.
9. J.H. Wood *et al.*, ASME Paper No. 82-GT-99, April, 1982.
10. J.H. Wood *et al.*, ASME Paper No. 85-GT-9, March, 1985.
11. L.F. Aprigliano, Department of the Navy Report No. DTNSRCD/SME-81/10 June, 1981.
12. J.R. Vargas, in: "Metallurgical Coatings 80", Conference Proceedings, San Diego, CA, Vol. II, J.N. Zemel (ed.), Elsevier Sequoia, Lausanne, April 1980, p. 407.
13. J.J. Grisik *et al.*, *ibid.*, p. 397.
14. M. Villat and P. Felix, *Sulzer Tech. Rev.*, p. 97 (March 1976).
15. R.J. Pennisi and D.K. Gupta, NASA Cr-165234, 1981.
16. S. Mrowec, T. Walec and T. Werber, *Oxid. Met.*, **1**(1), 93 (1969).
17. E.J. Vineberg and D.L. Douglass, *Oxid. Met.*, **25**(1/2), 1 (1986).
18. S. Mrowec and M. Wedrychowska, *Oxid. Met.*, **13**, 481 (1979).
19. E.M. Jalloulli, J.P. Larpin, M. Lambertin and J.C. Colson, *J. Electrochem. Soc.*, **126**, 2254 (1979).
20. S. Mrowec, S. Tochowicz, T. Werber and J. Podhorodecki, *Corrosion Sci.*, 7, 697 (1967).
21. T. Narita, K. Przybylski and W.W. Smeltzer, *Oxid. Met.*, **22**(3/4), 181 (1984).
22. T. Biegun and A. Bruckman, *Bull. Acad. Polon. Sci. Ser. Sci. Chim.*, **28**, 377 (1980).
23. T. Biegun and A. Bruckman, *Bull. Acad. Polon. Sci. Ser. Sci. Chim.*, **29**, 69 (1981).
24. E. Godlewska, K. Godlewski, S. Mrowec and M. Danielewski, *Mat. Sci. & Eng.*, **A120**, 105 (1989).
25. E. Godlewska, K. Godlewski and S. Mrowec, *Mat. Sci. & Eng.*, 87, 183 (1987).
26. V.I. Kovaliv, J.A. Kesler, I.V. Gordeev, J.D. Trietiakov and P.M. Mielnik, *Izv. Akad. Nauk. SSSR, Neorg. Mat.*, **17**, 2084 (1981).
27. E. Godlewska and S. Mrowec (in print), 1992.